Journal of Alloys and Compounds, 210 (1994) 213–220
JALCOM 1132

Neutron diffraction studies of $LaMn_2Ge_2$ and $LaMn_2Si_2$ compounds: evidence of dominant antiferromagnetic components within the Mn planes

G. Venturini[a], R. Welter[a], E. Ressouche[b] and B. Malaman[a,*]

[a]*Laboratoire de Chimie du Solide Minéral, Université de Nancy I, associé au CNRS, UA 158, B.P. 239, 54506 Vandoeuvre les Nancy Cedex (France)*

[b]*CEA/Département de Recherche Fondamentale sur la Matière Condensée/SPSMS-MDN, 17 rue des Martyrs, 38054 Grenoble Cedex 9, (France)*

(Received January 4, 1994)

Abstract

The magnetic properties of $ThCr_2Si_2$-type structure $LaMn_2Ge_2$ and $LaMn_2Si_2$ compounds have been reinvestigated by neutron diffraction experiments. The ferromagnetic ordering previously proposed to take place on the manganese sublattice is revised. At high temperature, both compounds are purely collinear antiferromagnets (not detected by magnetic measurements), characterized by a stacking of antiferromagnetic (001) Mn planes. Below $T_c = 310$ and 325 K for $LaMn_2Ge_2$ and $LaMn_2Si_2$, respectively, both compounds exhibit an easy-axis ferromagnetic behaviour. However, the occurrence of a dominant antiferromagnetic component within the (001) Mn planes yields a conical magnetic structure for the germanide (cone semi-angle $\alpha = 58°$ at 2 K) and a canted magnetic structure for the silicide ($\phi = 49°$). At 2 K, the total Mn moments are about 3.0 and 2.4 μ_B for $LaMn_2Ge_2$ and $LaMn_2Si_2$, respectively. The results are compared with those of closely related RMnSi and RMnGe compounds and the magnetic properties of the $ThCr_2Si_2$-type structure RMn_2X_2 (X≡Si, Ge) compounds are discussed.

1. Introduction

$LaMn_2Ge_2$ and $LaMn_2Si_2$ crystallize in the tetragonal $ThCr_2Si_2$-type structure (*I4/mmm*) [1]. The bulk magnetic properties of both compounds have been extensively studied in the last 20 years. Narasimhan *et al.* [2, 3] and Szytula and coworkers [4, 5] have studied their magnetic behaviour in powder samples while a single-crystal study of $LaMn_2Ge_2$ has been undertaken by Shigeoka *et al.* [6]. All these authors obtained similar ferromagnetic behaviour with Curie temperatures of about 303–310 and 306–326 K for $LaMn_2Si_2$ and $LaMn_2Ge_2$ respectively and a magnetization value per manganese atom of $\mu_{Mn} \approx 1.5$ μ_B at 4.2 K, for both compounds. However, it should be noticed that a higher Mn moment value (*i.e.* 2.1 μ_B) was derived by Ishida *et al.* [7] from electronic structure calculations for $LaMn_2Ge_2$.

From knowledge of the structurally related CeFeSi-type (*P4/nmm*) equiatomic rare-earth manganese silicides and germanides RMnX (R≡La–Sm, Gd) [8, 9], we found that compounds with Mn–Mn intralayer distances greater than about 2.85 Å were characterized by antiferromagnetic Mn layers. Bearing this criterion in mind, a recent neutron diffraction study of $CaMn_2Ge_2$ and $BaMn_2Ge_2$ ($d^a_{Mn-Mn} = 2.93$ and 3.14 Å respectively) [10] led us to discover the first $ThCr_2Si_2$-type manganese compounds characterized by antiferromagnetic Mn layers. The Mn moment values are much higher than that observed in $LaMn_2Ge_2$, *i.e.* $\mu_{Mn} = 3.66$, 2.67 and 1.5 μ_B for $BaMn_2Ge_2$, $CaMn_2Ge_2$ and $LaMn_2Ge_2$ respectively. Bearing in mind the Mn–Mn intralayer spacings in the isotypic lanthanum manganese silicide and germanide, we decided to undertake a neutron diffraction study of these compounds. Indeed, the occurrence of an antiferromagnetic component within the (001) Mn planes would also explain the surprisingly low values of the Mn moments observed in both compounds.

2. Experimental procedures

The compounds were prepared from commercially available high-purity elements. Pellets of stoichiometric mixture were compacted using a steel die, and then introduced into silica tubes sealed under argon (100 mmHg). The samples were first heated at 1173 K for preliminary homogenization treatment and then melted

*Author to whom correspondence should be addressed.

0925-8388/94/$07.00
SSDI 0925-8388(94)01132-2

in an induction furnace. Purity of the final sample was checked by powder X-ray diffraction (Guinier Cu Kα).

The magnetic measurements were carried out on a Faraday balance (above 300 K) and on a MANICS magneto-susceptometer (between 4.2 and 300 K), in fields up to 1.5 T.

Neutron diffraction experiments were carried out at the Siloe Reactor of the Centre d'Etude Nucléaire de Grenoble. Several patterns have been collected in the temperature range 2–313 K with the one-dimension curved multidetector DN5 ($\lambda = 2.4965$ Å). In order to correct for texture effects, following a procedure described in ref. 11, we used during the refinements a fitted coefficient (r_{cor}) which reflects the importance of preferential orientation. The values of r_{cor} obtained (see below) strongly support the validity of this correction.

Using the scattering lengths $b_{Si} = 4.149$ fm, $b_{Ge} = 8.185$ fm, $b_{Mn} = -3.73$ fm, $b_{La} = 8.29$ fm and the form factor of Mn from ref. 12, the scaling factor, the $z_{Ge,Si}$ atomic positions, r_{cor} and the Mn magnetic moments were refined by the mixed crystallographic executive for diffraction (MXD) least-squares fitting procedure [13]. The MXD program allows simultaneous fitting of the calculated nuclear and magnetic intensities to the observed ones.

In the $ThCr_2Si_2$-type structure (space group *I4/mmm*), the rare-earth and silicon (germanium) atoms occupy the 2(a) (0,0,0) and 4(e) (0,0,z) with $z \approx 0.38$ sites respectively. The manganese atoms occupy the special position 4(d): (0,1/2,1/4) with an additional C translation mode. Thus, it is important to stress that the magnetic contributions to the observed intensities, due to a ferromagnetic ordering of the Mn sublattice, affect only the nuclear lines obeying the limiting reflection condition: (*hkl*) with $h+k=2n$. On the contrary, in each case, attempts made to fit the nuclear lines by interchanging the position of the Mn and Si(Ge) atoms always led to a poorer agreement and gave no evidence for any mixing between Mn and Si(Ge) atoms in 4d and 4e sites.

3. Magnetic measurement

The temperature dependence of the susceptibility measured in the temperature range 4.2–600 K (Fig. 1) yields Curie temperatures of approx. 325 K and approx. 310 K for $LaMn_2Ge_2$ and $LaMn_2Si_2$, respectively. The paramagnetic Curie temperatures, the effective magnetic moment values and the maximum magnetization values at 4.2 K (Table 1) are in good agreement with previous published data [2–7, 14].

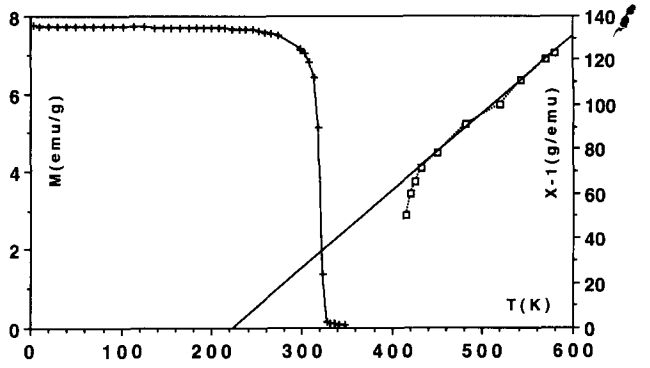

Fig. 1. Temperature dependence of magnetization ($H_{app} = 500$ Oe) and inverse susceptibility ($H_{app} = 5$ kOe) in $LaMn_2Ge_2$.

TABLE 1. Magnetic data for $LaMn_2Ge_2$ and $LaMn_2Si_2$

Compound	T_c (K)	θ_p (K)	$\mu_{eff.}$ (μ_B)	M (4.2 K, 15 kG) (μ_B)
$LaMn_2Ge_2$	325	225	3.39	1.45
$LaMn_2Si_2$	310	254	3.10	1.55

4. Neutron diffraction study

4.1. $LaMn_2Ge_2$

The neutron diffraction patterns (Fig. 2) are similar over the whole temperature range studied (2–313 K) and are characterized by two kinds of magnetic contributions.

The first ones occur only for nuclear peaks which obey the rule: (*hkl*) with $h+k=2n$ and are characteristic of ferromagnetic (001) Mn planes (see section 2). Since the I translation mode remains, the resulting magnetic arrangement corresponds to a stacking along the c-axis of ferromagnetically coupled ferromagnetic (001) Mn planes. The absence of a magnetic contribution to the (00*l*) reflections indicates that the moments are along the [001] direction.

The other magnetic contributions are evidenced by several superlattice reflections. The Bragg angle values are consistent with an incommensurate magnetic ordering. They may be indexed as satellites of the "(*hkl*) with $h+k=2n+1$" nuclear lines with a wavevector $\boldsymbol{k} = (0,0,q_z)$. In addition, the calculation of q_z indicates a thermal variation of this value (from 0.294 to 0.260 between 313 and 2 K) reported on Fig. 3. These results suggest the occurrence of a helical component with a propagation direction along the c-axis. Furthermore, the extinction rules (see Table 2) imply that the corresponding Mn moment components are antiferromagnetically coupled within the (001) planes, *i.e.* with a phase angle difference of 180° while the phase angle between the atoms related by the I translation is 0°. Under these conditions, the magnetic structure is a

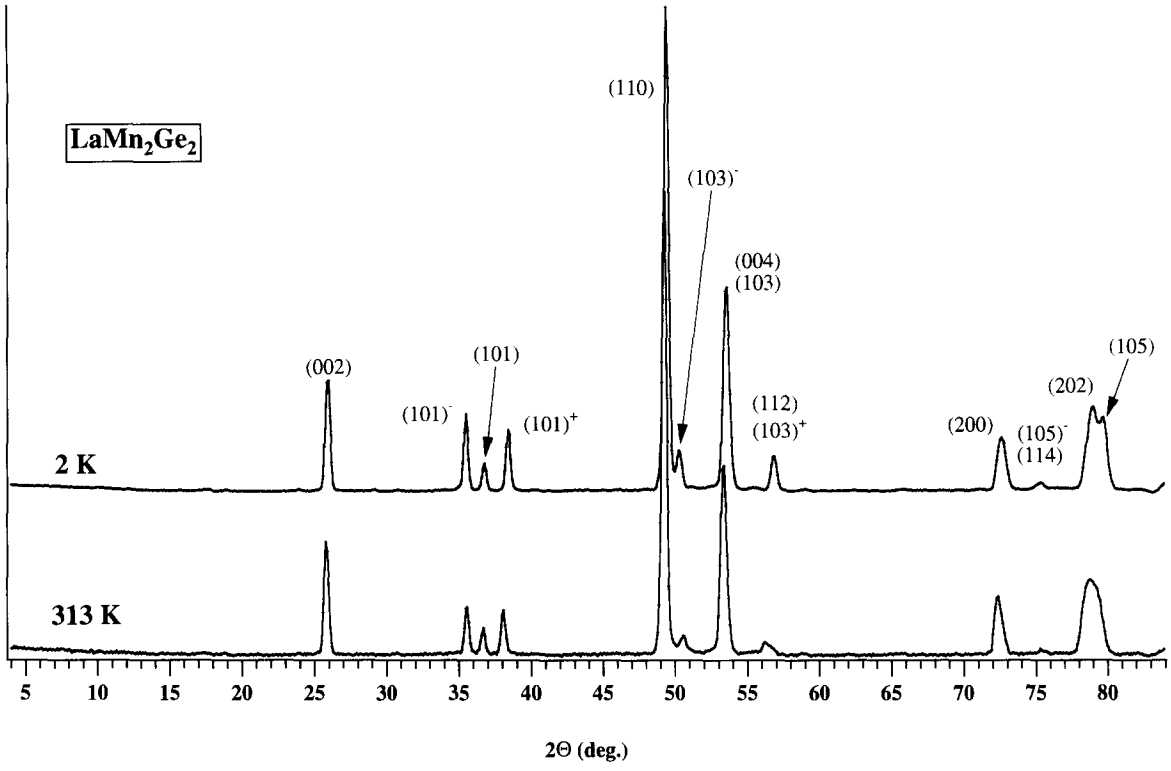

Fig. 2. Neutron diffraction patterns of $LaMn_2Ge_2$ at 2 and 313 K.

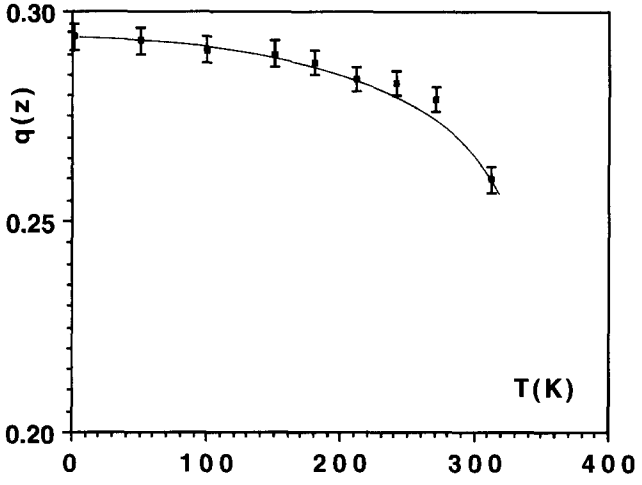

Fig. 3. Temperature dependence of the q_z component of the wavevector in $LaMn_2Ge_2$.

conical one, as shown in Fig. 4. At 2 K, the best refinement leads to 2.6(4) μ_B and 1.61(11) μ_B for the helical and ferromagnetic components respectively, yielding a cone semi-angle (α) of approx. 58° (Table 2). As shown in Fig. 4, the modulation vector of 0.260 (in units of the τ_{00l} reciprocal lattice vector) corresponds to a helical-turn angle of about $\pm 47°$ between adjacent layers for the Mn atoms related by the I translation mode yielding a repeat distance of about 71 Å. The total resulting Mn moment of about 3 μ_B per atom is much higher than that found by magnetization measurements (Table 1). The thermal variation of each component is plotted in Fig. 5. It is noteworthy that the value of the ferromagnetic component strongly decreases between 2 and 313 K (Table 2) and vanishes at $T_c \approx 322$ K, in good accordance with the thermal variation of the susceptibility. On the other hand, the value of the helimagnetic component decreases slightly in the same temperature range (Table 2). The shape of the corresponding curve (Fig. 5) clearly suggests that the ordering temperature T_t, not detected in the bulk susceptibility measurements, might be much higher than the Curie temperature. Between T_c and T_t, the magnetic structure would probably be characterized by a flat spiral or a collinear antiferromagnetic arrangement as observed in $LaMn_2Si_2$ (see below). Nevertheless, a neutron diffraction study above room temperature would be helpful to characterize this hypothetical magnetic ordering and give an estimate of T_t.

The magnetic structure is shown in Fig. 4. Table 2 gives the observed and calculated intensities together with the lattice constants and the various adjustable parameters at 313 and 2 K.

4.2. $LaMn_2Si_2$

Neutron diffraction patterns recorded at 315, 50 and 2 K are shown in Fig. 6. Three steps have to be considered.

TABLE 2. Calculated and observed intensities, lattice constants and adjustable parameters in $LaMn_2Ge_2$ at 313 and 2 K

hkl	313 K		2 K	
	I_c	I_o	I_c	I_o
002	64.2	63.6(6)	65.9	65.2(7)
101^-	44.7	45.2(8)	61.3	62.9(8)
101	20.7	24.3(6)	21.1	24.1(8)
101^+	48.2	47(1)	66.6	64(1)
110	889.6	883(4)	909.5	906(5)
103^-	34.7	41(1)	48.1	61(1)
004				
103	475.7	497(7)	470.6	496(7)
103^+	34.3	17(1)		
112	16.9	27(1)	86.7	85(2)
200	255.9	269(7)	269.7	288(9)
105^-			28.0	45(2)
114	23.5	25(2)	13.3	19(2)
202	436.8	454(6)	463.3	448(7)
105	465.1	452(6)	477.1	472(7)
a (Å)	4.204(2)		4.190(3)	
c (Å)	10.996(6)		10.948(9)	
q_z	0.260(2)		0.294(3)	
r_{cor}	1.15(1)		1.15(1)	
z_{Ge}	0.380(1)		0.380(1)	
μ_{Mn}(F) (μ_B)[a]	0.87(19)		1.61(11)	
μ_{Mn}(H) (μ_B)[b]	2.22(5)		2.60(4)	
μ_{Mn}(total) (μ_B)	2.38(9)		3.06(5)	
R(%)	2.9		3.3	

[a]F, ferromagnetic.
[b]H, helimagnetic.

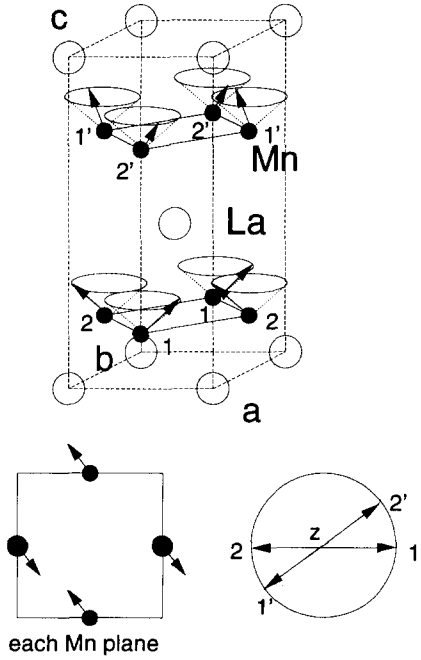

Fig. 4. Magnetic structure of $LaMn_2Ge_2$ at 2 K.

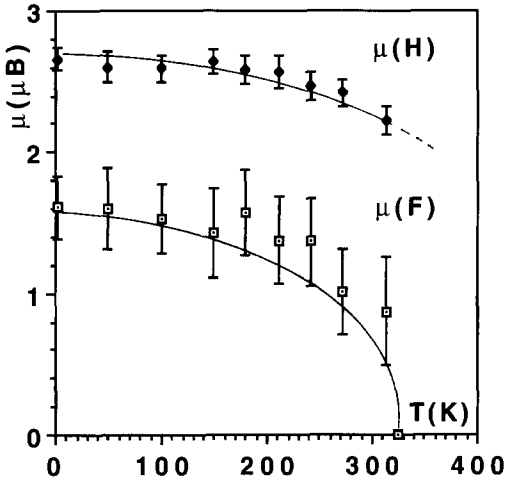

Fig. 5. Temperature dependence of the ferromagnetic (F) and helimagnetic (H) components of the manganese moments in $LaMn_2Ge_2$.

4.2.1. $T = 315$ K

At this temperature, *i.e.* above the Curie point (Table 1), the pattern shows magnetic contributions only for nuclear lines which obey the rule: (hkl) with $h+k=2n+1$ (Fig. 6). This is particularly obvious for the (101) line for which the observed intensity is much greater than the purely nuclear calculated one. This result indicates an anti-*C* ordering, giving evidence of an antiferromagnetic arrangement of the Mn moments within the (001) planes. The best refinements lead to moments aligned along the *c*-axis and give a Mn moment value of 1.2 μ_B (Table 3). Similar magnetic arrangements have been observed in $CaMn_2Ge_2$ and $BaMn_2Ge_2$ [10]. The magnetic structure is sketched in Fig. 7(a). It consists of a stacking of antiferromagnetic (001) Mn layers. The manganese moments are antiferromagnetically coupled with their direct neighbours situated in each adjacent plane along the *c*-axis, in agreement with the remaining *I* translation mode (Table 3). As in the case of $LaMn_2Ge_2$, it is noteworthy that this magnetic behaviour is not detected in the bulk susceptibility measurements. Therefore, a neutron diffraction study, above room temperature, would be necessary to determine the corresponding Néel temperature.

4.2.2. $315 < T < 40$ K

Below 310 K, the intensities of the previous lines increase, and new magnetic contributions to the intensities of the nuclear reflections which obey the rule (hkl) with $h+k=2n$ are observed. This is particularly obvious for the (112) line for which the nuclear contribution has an almost-zero net value (Table 3). This implies that an additional ferromagnetic (see section 2) ordering occurs on decreasing the temperature, in agreement with the magnetometric measurements. From

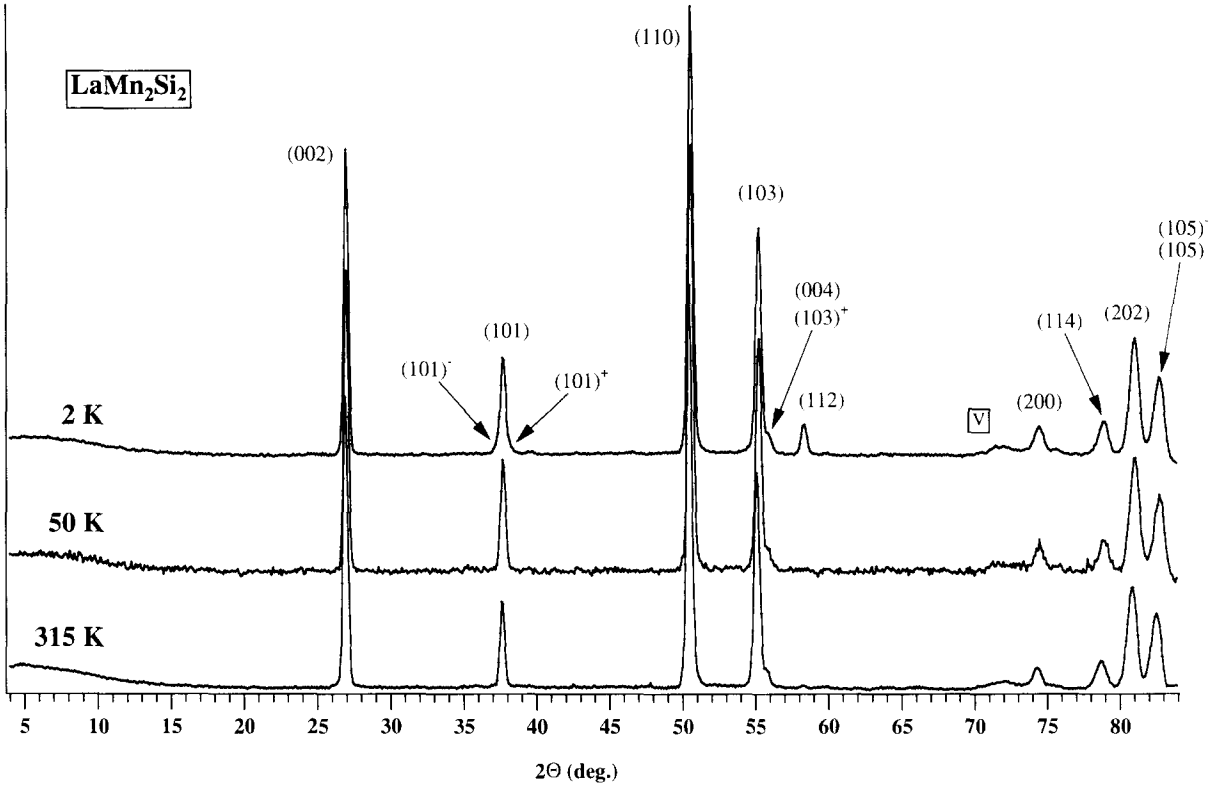

Fig. 6. Neutron diffraction patterns of $LaMn_2Si_2$ at 2, 50 and 315 K.

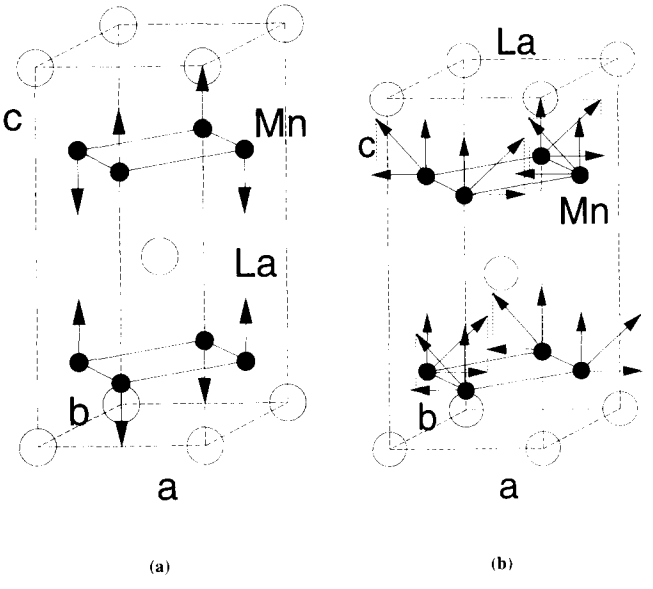

Fig. 7. Magnetic structures of $LaMn_2Si_2$ at (a) 315 K and (b) 50 K.

these observations, refinements were performed to account for the following magnetic model: a canted ferromagnetic structure in which the Mn moments are antiparallel to each other in the (001) planes and are canted between the Mn sublayers. The antiferromagnetic component lies in the (001) planes whereas the ferromagnetic component is parallel to the c-axis (Fig. 7(b)). The final refinement leads to a residual factor $R=4.6\%$ (Table 3). At 50 K, the canting angle of the Mn moment from the c-axis is $\alpha=49°$. The thermal dependence of each magnetic component (Fig. 8) gives a ferromagnetic ordering temperature of $T_c \sim 308$ K, in fair agreement with the magnetometric measurements. The total resulting Mn moment is found to be $\mu_{Mn}=2.44\ \mu_B$ per atom, which value is much higher than that found by magnetization measurements (Table 1).

4.2.3. $T<40$ K

Below 40 K, the (101) line intensity slightly decreases and two contributions, which remain weak down to 2 K, appear at the foot of this line. These additional lines can be indexed as satellites of the (101) line with a wavevector $\boldsymbol{k}=(0,0,q_z)$. The value of q_z is estimated to be 0.09 at 2 K. As in the case of $LaMn_2Ge_2$ (see above), these results are consistent with the occurrence of a conical magnetic arrangement. Nevertheless, since the magnetic contribution to the intensity of the (101) reflection never completely vanishes, we have to conclude that the canted and the conical magnetic structures coexist down to 2 K. Under these conditions, the refinements lead to a helical magnetic component of about 0.8 μ_B and a cone semi-angle of 25°, the total magnetic Mn moment remaining quite constant (2.43

TABLE 3. Calculated and observed intensities, lattice constants and adjustable parameters in $LaMn_2Si_2$ at 315, 50 and 2 K

hkl	315 K		50 K		2 K	
	I_c	I_o	I_c	I_o	I_c	I_o
002	97.9	97.6(2)	99.6	100.2(4)	95.6	95.3(3)
101^-	0	0	0	0	6.2	6.5(4)
101	52.3	52.3(3)	75.8	76.9(6)	61.6	61.9(3)
101^+	0	0	0	0	6.3	5.8(4)
110	468	463(2)	511	507(2)	512	491(2)
103^-						
103	311	308(2)	340	336(3)	342	316(4)
103^+						
004	21.0	24.7(4)	19	31(3)	23	37(3)
112	2.0	2.3(4)	49	47(1)	49	45(1)
200	67	75(2)	89	94(3)	89	103(2)
114	86	108(3)	104	125(3)	102	130(1)
202	409	460(2)	464	480(4)	447	460(3)
105^-						
105	330	323(3)	383	359(5)	353	327(3)
a (Å)	4.120(1)		4.112(1)		4.112(1)	
b (Å)	10.626(2)		10.601(2)		10.600(3)	
q_z	0		0		0.089(2)	
r_{cor}	1.02(1)		1.03(1)		1.02(1)	
z_{Ge}	0.378(2)		0.381(2)		0.378(4)	
μ_{Mn}(F) (μ_B)[a]	0		1.59(14)		1.61(14)	
μ_{Mn}(C) (μ_B)[b]	1.20(5)		1.85(9)		1.64(8)	
μ_{Mn}(H) (μ_B)[c]	0		0		0.79(26)	
μ_{Mn}(AF) (μ_B)	1.20(5)		1.85(9)		1.82(14)	
μ_{Mn}(total) (μ_B)	1.20(5)		2.44(12)		2.43(15)	
R(%)	3.7		4.6		6.5	

[a]F, ferromagnetic.
[b]C, collinear.
[c]H, helimagnetic.

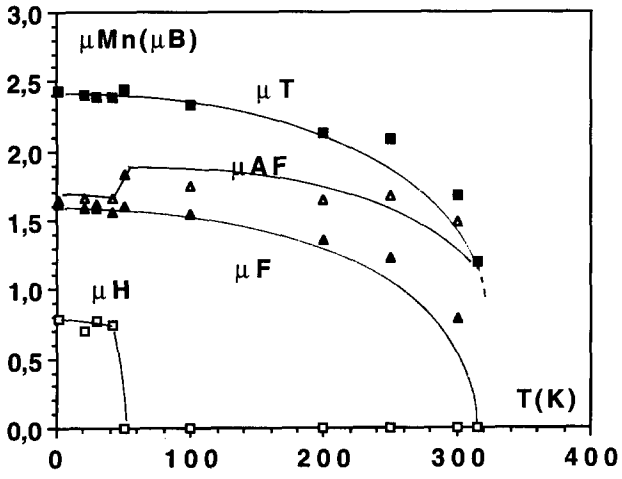

Fig. 8. Temperature dependence of the ferromagnetic (F), antiferromagnetic (AF) and helimagnetic (H) components of the Mn moments in $LaMn_2Si_2$.

μ_B). The thermal dependence of each magnetic component (Fig. 8) gives an ordering temperature T_t of about 45 K.

Table 3 gives the observed and calculated intensities together with the lattice constants and the various adjustable parameters at 315, 50 and 2 K.

5. Discussion

The main result provided by this study is the occurrence of new HT antiferromagnetic structures for $LaMn_2Si_2$ and $LaMn_2Ge_2$. Moreover, below about 310 K, an easy-axis ferromagnetic state characterized by large antiferromagnetic components within the (001) Mn planes occurs for both compounds. This behaviour implies a new analysis of the magnetic behaviour of this class of compounds.

First, the Mn moment values deduced from the neutron diffraction data are now in fair agreement with those observed in isotypic $NdMn_2Si_2$ and $NdMn_2Ge_2$ compounds (as reported in refs. 2–7 and this work). In both compounds, the reduced values deduced from all the magnetization measurements recorded at 4.2 K (see refs. 1–5 and this work) correspond only to the ferromagnetic component of their magnetic structures,

the antiferromagnetic component being obscured at least below $H_{appl.} = 5$ T [6].

Furthermore, the total Mn moments in both compounds, deduced from the present study, account well for the hyperfine field values obtained by Sampathkumaran *et al.* [16] from ^{55}Mn nuclear magnetic resonance (NMR) experiments. There is fair agreement between the ratio of the Mn moments measured by neutron diffraction and the ratio of the hyperfine fields measured by NMR:

$$\frac{\mu_{Mn}(LaMn_2Si_2)}{\mu_{Mn}(LaMn_2Ge_2)} = \frac{2.43\ \mu_B}{3.03\ \mu_B} = 0.79$$

$$\frac{H^{Hyp}_{Mn}(LaMn_2Si_2)}{H^{Hyp}_{Mn}(LaMn_2Ge_2)} = \frac{164\ kOe}{200.3\ kOe} = 0.82$$

Moreover, according to the occurrence of an incommensurate magnetic component in $LaMn_2Ge_2$, the apparent crystallographic disorder noted by Sampathkumaran *et al.* [16] in the NMR spectra of the germanide probably originates from a distribution of Mn sites due to the different orientations of the hyperfine fields with respect to the principal axis of the electric field gradient.

Nevertheless, for this compound, the discrepancies between the Mn moment values derived from electronic structure calculations ($\mu_{Mn} = 2.1\ \mu_B$) [7] and measured by neutron diffraction ($\mu_{Mn} = 3\ \mu_B$) (this work) remain unexplained.

The second point concerns the values of the Mn moments in $LaMn_2Si_2$ and $LaMn_2Ge_2$, where the higher value is observed in the latter compound. Moreover, despite the larger unit cell of the germanide, this compound shows the higher ordering temperature. Similar effects are observed in the equiatomic RMnX (R = alkaline and rare earths, X = elements of groups 15 and 16) [8, 9, 17, 18]. Muller *et al.* [18] have shown that they have to be correlated with the Mn–X distances and the nature of this bond. It is noteworthy that such effects influence also the strength of the magnetic interactions, yielding an increase of the transition temperatures with an increase of the Mn moment value. This behaviour has been discussed at length in ref. 8.

The next point relates to the dominant antiferromagnetic Mn–Mn intralayer couplings observed in both $LaMn_2Si_2$ and $LaMn_2Ge_2$ compounds. The antiferromagnetic coupling is identical to those found in the corresponding alkaline-earth germanides [10]. Under these conditions, the magnetic behaviour of these $ThCr_2Si_2$-type compounds has to be related to that occurring in the CeFeSi-type RMnSi silicides and germanides. In these RMnSi(Ge) series we have emphasized that antiferromagnetic (001) Mn planes occur when the Mn–Mn intralayer separation is larger than approx. 2.85 Å, *i.e.* for R≡La–Nd. Ferri- or ferromagnetic behaviour is observed in GdMnSi [19] and YMnSi [20] where the Mn–Mn distances are lower than this critical distance. It is very interesting to note that this criterion is fulfilled for $LaMn_2Si_2$ and $LaMn_2Ge_2$, at least at high temperature, as well as for $CaMn_2Ge_2$ and $BaMn_2Ge_2$ [10]. Moreover, it is noteworthy that the same phenomenon occurs in the other RMn_2Ge_2 with $d^a_{Mn-Mn} > 2.85$ Å, *i.e.* for compounds in which R = Ce, Pr, Nd, Sm, previously described as purely ferromagnetic [21]. According to the antiferromagnetic behaviour of SmMnSi ($d_{Mn-Mn} = 2.86$ Å) and the ferrimagnetic behaviour of GdMnSi ($d_{Mn-Mn} = 2.84$ Å), the critical distance in the CeFeSi-type compounds seems to range from 2.86 to 2.84 Å. Within the $ThCr_2Si_2$ silicides, $LaMn_2Si_2$ ($d_{Mn-Mn} = 2.91$ Å) exhibits purely antiferromagnetic Mn planes at high temperature while $CeMn_2Si_2$ ($d_{Mn-Mn} = 2.85$ Å) [22] and $PrMn_2Si_2$ ($d_{Mn-Mn} = 2.85$ Å) [15] are characterized by ferromagnetic planes.

Until now, all the known magnetic structures of $ThCr_2Si_2$-type manganese silicides and germanides were said to be characterized by ferromagnetic (001) Mn planes, whatever the intralayer Mn–Mn spacings, stacked ferro- or antiferro-magnetically along the *c*-axis (for a long review, see ref. 5). Our results seriously question the correctness of the previous conclusions deduced from this observation since they show that, until now, no purely ferromagnetic structures occur in this class of compounds. Szytula *et al.* have pointed out for the first time that the intralayer Mn–Mn spacings have a close relationship to the appearance of AF or F states of the Mn sublattice: interatomic Mn–Mn distances greater than 2.85 Å lead to ferromagnetic interplane interactions, whereas distances lower than 2.85 Å lead to antiferromagnetic interplane interactions. In fact, the occurrence of antiferromagnetic planes at high temperature in $LaMn_2Si_2$ rather indicates that this effect is the main feature. The occurrence of ferromagnetism at lower temperature results of secondary effects. It does not seem to correlate with a critical interatomic distance since it appears at approximately the same temperature in both $LaMn_2Si_2$ and $LaMn_2Ge_2$ compounds characterized by different unit cell parameters. One may think that such antiferromagnetic (001) planes induce additional interplane ferromagnetic interactions which begin to act when the thermal contraction of the parameters smoothes the antiferromagnetic in-plane interactions. Moreover, the strength of these additional ferromagnetic interactions seems to be very sensitive to the electron concentration since they do not act in the corresponding alkaline-earth germanides. Such an effect might account for the negative pressure dependence of "T_c" observed by Taneko *et al.* [14] in $NdMn_2Ge_2$. Increasing the pressure might tend to locate the electrons along the interatomic bonds, yielding a lowering of the concentration of conduction

electrons. The purely antiferromagnetic behaviour of $CaMn_2Ge_2$, having the same unit cell volume and one electron less than $NdMn_2Ge_2$, strongly confirms this conclusion. Lastly, it is noteworthy that the occurrence of modulated magnetic ordering is a common characteristic of numerous intermetallic compounds, particularly in the case of manganese compounds such as MnSi or YMn_6Ge_6 [23]. Similar explanations [23] may perhaps apply to the present compounds, at least for those with diamagnetic rare-earth components.

6. Conclusions

Neutron diffraction study of $LaMn_2Si_2$ and $LaMn_2Ge_2$ has revealed the occurrence of a dominant antiferromagnetic component within the (001) Mn planes in these compounds, previously reported as collinear ferromagnets. Furthermore, this study leads to the more reasonable Mn moment values of 2.4 and 3 μ_B against the value 1.5 μ_B previously published. Such behaviour is also encountered in $Ca(Ba)Mn_2Ge_2$ and the equiatomic RMnSi(Ge) compounds. All these results lead to the conclusion that the magnetic order in the (001) Mn planes is related to the intralayer Mn–Mn distances and to the valency of the largest metal, whereas the Mn moment values are correlated with the nature of the Mn–X bond (Mn–X distances). The effect of ferromagnetic or antiferromagnetic planes on the interplane couplings is less clear, though the two effects seem to be correlated. From this point of view, it would be interesting to re-investigate the magnetic properties of the $SmMn_2Ge_2$ compound in the light of the present results.

Further investigations are necessary to complete this preliminary information. A neutron diffraction study of the other light rare-earth manganese germanides of the RMn_2Ge_2 series and the solid solution $La_xY_{1-x}Mn_2Ge_2$ may allow a better understanding of the influence of the Mn–Mn intralayer spacing on the exchange. This work is under way. Moreover, the influence of the R valency will be checked by magnetization measurements on solid solutions such as $La_xCa_yY_{1-x-y}Mn_2Ge_2$ where y is related to the mean valency and x is chosen to keep the Mn–Mn spacings constant.

References

1 P. Villars and L.D. Calvert, *Pearson's Handbook of Crystallography Data for Intermetallic Phases,* American Society for Metals, Materials Park, OH 2nd edn., 1991.
2 K.S.V.L. Narasimhan, V.U.S. Rao, R.L. Bergner and W.E. Wallace, *J. Appl. Phys., 46* (1975) 4957.
3 K.S.V.L. Narasimhan, V.U.S. Rao, W.E. Wallace and I. Pop, *AIP Conf. Proc., 29* (1975) 594.
4 A. Szytula and I. Szott, *Solid State Comm., 40* (1981) 199.
5 A. Szytula and J. Leciejewicz, Magnetic properties of ternary intermetallic compounds of the RT_2X_2 type, in K.A. Gschneidner Jr. and L. Eyring (eds.), *Handbook on the Physics and Chemistry of Rare Earths,* Vol. 12, Chapter 83, Elsevier Science Publishers, 1989, p. 133.
6 T. Shigeoka, N. Iwata, H. Fujii and T. Okamoto, *J. Magn. Magn. Mater., 53* (1985) 83.
7 S. Ishida, S. Asano and J. Ishida, *J. Phys. Soc. Jpn., 55*(3), (1986), 936.
8 R. Welter, G. Venturini, E. Ressouche and B. Malaman, *J. Alloys Comp., 206* (1994) 55.
9 R. Welter, G. Venturini, E. Ressouche and B. Malaman, *J. Alloys Comp.* (to be published).
10 R. Welter, G. Venturini, E. Ressouche and B. Malaman, *J. Alloys Comp.* (to be published).
11 R. Welter, G. Venturini and B. Malaman, *J. Alloys Comp., 189* (1992) 49.
12 C.G. Shull and Y. Yamada, *J. Phys. Soc. Jpn., 22* (1962) 1210.
13 P. Wolfers, *J. Appl. Crystallogr., 23* (1990) 554.
14 K. Taneko, H. Yasui, T. Kanomata and T. Suzuki, *J. Magn. Magn. Mater., 104–107* (1992) 1951.
15 R. Welter, G. Venturini, D. Fruchart and B. Malaman, *J. Alloys Comp., 191* (1993) 263.
16 E.V. Sampathkumaran, L.C. Gupta, R. Vijayaraghavan, Le Dang Khoi and P. Veillet, *J. Phys. Met. Phys., 12* (1982) 1039.
17 W. Bronger, P. Muller, R. Hoppner and H.U. Schuster, *Z. Anorg. Allg. Chem., 539* (1986) 175.
18 R. Muller, M. Kuckel, H.U. Schuster, P. Muller and W. Bronger, *J. Alloys Comp., 176* (1991) 167.
19 S.A. Nikitin, T.I. Ivanova, O.V. Nekrasova, R.S. Torchinova, Yu.F. Popov, O.N. Koryasova and Ye. A. Klyucnikova, *Fiz. Metal., Metaloved., 64*(6) (1987) 1071.
20 H. Kido, T. Hoshikawa, M. Tagami, M. Shimada and M. Koizumi, *J. Ceram. Assoc. Jpn., 94*(1) (1986) 232.
21 R. Welter, G. Venturini, E. Ressouche and B. Malaman, *J. Alloys Comp.* (to be published).
22 S. Siek, A. Szytula and J. Leciejewicz, *Phys. Stat. Sol. (a), 46* (1978) K101.
23 G. Venturini, R. Welter and B. Malaman, *J. Alloys Comp., 200* (1993) 51.